Extracellular ATP induces oscillations of intracellular Ca^{2+} and membrane potential and promotes transcription of IL-6 in macrophages

Peter J. Hanley*†, Boris Musset*†, Vijay Renigunta*†, Sven H. Limberg*†, Alexander H. Dalpke†‡, Rainer Sus*, Klaus M. Heeg‡, Regina Preisig-Müller*, and Jürgen Daut*§

*Institute of Physiology, Marburg University, Deutschhausstrasse 2, 35037 Marburg, Germany; and ‡Institute of Microbiology, Marburg University, Pilgrimstein 2, 35037 Marburg, Germany

Edited by Erwin Neher, Max Planck Institute for Biophysical Chemistry, Goettingen, Germany, and approved May 10, 2004 (received for review February 2, 2004)

The effects of low concentrations of extracellular ATP on cytosolic Ca^{2+}, membrane potential, and transcription of IL-6 were studied in monocyte-derived human macrophages. During inflammation or infection many cells secrete ATP. We show here that application of 10 μM ATP or 10 μM UTP induces oscillations in cytosolic Ca^{2+} with a frequency of $\approx$12 min^{-1} and oscillations in membrane potential. RT-PCR analysis showed expression of $P2Y_1$, $P2Y_2$, $P2Y_{11}$, $P2X_1$, $P2X_4$, and $P2X_7$ receptors, large-conductance (*KCNMA1* and *KCNMB1–4*), and intermediate-conductance (*KCNN4*) Ca^{2+}-activated K^+ channels. The Ca^{2+}oscillations were unchanged after removal of extracellular Ca^{2+}, indicating that they were mainly due to movements of Ca^{2+} between intracellular compartments. Comparison of the effects of different nucleotides suggests that the Ca^{2+} oscillations were elicited by activation of $P2Y_2$ receptors coupled to phospholipase C. Patch–clamp experiments showed that ATP induced a transient depolarization, probably mediated by activation of $P2X_4$ receptors, followed by membrane potential oscillations due to opening of Ca^{2+}-activated K^+ channels. We also found that 10 μM ATPγS increased transcription of IL-6 $\approx$40-fold within 2 h. This effect was abolished by blockade of P2Y receptors with 100 μM suramin. Our results suggest that ATP released from inflamed, damaged, or metabolically impaired cells represents a ''danger signal'' that plays a major role in activating the innate immune system.

Macrophages are one of the key cellular components of the innate immune system. They interact with the adaptive immune system by means of two signals: (*i*) a signal generated by the presentation of antigens to specific T cells, and (*ii*) a signal generated by presentation of costimulatory molecules, such as CD80 and CD86, to T cells (1, 2). The costimulatory molecules are presented at the surface of macrophages after interaction of intracellular or extracellular pattern recognition receptors with pathogen-associated molecular patterns (''infectious nonself'' signals). It is generally assumed that the adaptive immune system responds to antigens only if both signals are present (''infectious nonself model''), but the signal transduction mechanisms are still under debate (1–3). The infectious nonself model implies that the innate immune system controls the adaptive immune system in the sense that it determines whether the adaptive immune system responds to a nonself ligand.

In addition, it has recently been proposed that the antigen-presenting cells of the innate immune system respond preferentially to antigens perceived to be associated with a dangerous situation such as infection, injury or mechanical damage (''danger model'') (4, 5), which implies that a third signal (''danger signal'') may be required to fully activate the adaptive immune system. The danger model is based on the observation that substances released by lytic cells or by cells suffering from metabolic, infectious, or mechanical impairment (for example, CD40 ligand, heat shock proteins, or IFN-α) can induce ''activation'' of macrophages (4, 5). Here, we report that ATP induces oscillations of Ca^{2+} and membrane potential in macrophages and promotes transcription of IL-6. Our data suggest that an increase in extracellular ATP may represent a danger signal that plays a major role in activating the innate immune system.

ATP leaks out as a consequence of cell damage or acute cell death, but it can also be secreted by many cell types through nonlytic mechanisms, for example, during mechanical stimulation or metabolic stress, and even in the absence of an external stimulus (6–8). Purine and pyrimidine nucleotides control various cellular functions by activating P2X receptors, which are ligand-gated ion channels, and P2Y receptors, which are heptahelical G protein-coupled receptors (7, 9). Macrophages use purinergic receptors as indicators of cell and tissue damage and migrate toward sources of extracellular ATP (10, 11). Furthermore, extracellular ATP induces permeabilization of the cell membrane to large molecules, activation of lipopolysaccharide-stimulated macrophages, and the release of cytokines (12, 13). All of these effects were observed at ATP concentrations between 100 and 1,000 μM. Even higher concentrations of ATP are required to induce apoptosis of macrophages and the killing of ingested bacteria (14). However, *in vivo* extracellular ATP is rapidly hydrolyzed by ectonucleotidases, and extracellular concentrations have been estimated to be $<$25 μM (8). Relatively few studies have addressed the effects of low concentrations of ATP on macrophages. In murine peritoneal macrophages, 10–100 μM ATP was found to induce a transient rise in intracellular Ca^{2+} that was insensitive to extracellular Ca^{2+} and was thought to reflect a second messenger-operated Ca^{2+} release from the endoplasmic reticulum (15). In the same cell type, local application of ATP or UTP through microelectrodes was found to induce a transient inward current followed by an outward current (16). In the present study, we sought to obtain more information on the role of extracellular ATP in macrophage physiology.

Materials and Methods

Human Macrophage Cultures. Peripheral blood mononuclear cells were prepared by density centrifugation (Ficoll/Hypaque, 1.077 g·ml^{-1}, Biochrom, Berlin) from the blood of healthy adult volunteers. Peripheral blood mononuclear cells were plated in cell culture dishes containing glass cover slips in Clicks/RPMI medium 1640 supplemented with 2 mM L-glutamine, 100 units·ml^{-1} penicillin, 100 μg·ml^{-1} streptomycin, and 10% heat-inactivated FCS (all from Biochrom). Macrophages for electrophysiological and fluorescence

This paper was submitted directly (Track II) to the PNAS office.

Abbreviations: IK_{Ca}, Ca^{2+}-activated K^+; M-CSF, macrophage-colony-stimulating factor.

Data deposition: The sequence reported in this paper has been deposited in the GenBank database (accession no. AY445624).

†P.J.H., B.M., V.R., S.H.L., and A.H.D. contributed equally to this work.

§To whom correspondence should be addressed. E-mail: jdaut@staff.uni-marburg.de.

measurements were prepared by culturing the peripheral blood mononuclear cells in the presence of 5 ng·ml^{-1} recombinant human macrophage-colony-stimulating factor (M-CSF) (PeproTech, Rocky Hill, NJ) for 2 weeks. Macrophages of maximal purity for RT-PCR were isolated by positive selection with anti-CD14-MicroBeads (Miltenyi Biotec, Bergisch Gladbach, Germany) in a SuperMACS, following the manufacturer's protocol. Cells were then seeded at a density of 1×10^6 cells per ml in 12-well tissue culture plates and differentiated in medium containing M-CSF. The purity of isolation was >95% for CD14 expression. PCR analysis of receptors and ion channels and quantitative PCR of IL-6 were carried out with intron-spanning primers that are listed in Table 1, which is published as supporting information on the PNAS web site.

Measurement of Intracellular Ca^{2+} and Na^+. A coverslip with macrophages was sealed onto the bottom of a Perspex bath mounted on the stage of an inverted Nikon Diaphot 300 microscope. Cells were superfused with physiological salt solution containing 5% BSA and (in mM): 140 NaCl, 5.4 KCl, 1 $MgCl_2$, 0.33 NaH_2PO_4, 5 Hepes, 1 $CaCl_2$, and 10 glucose (pH, 7.4). Fluo-3/AM or Sodium green tetra-acetate (Molecular Probes) were first dissolved in anhydrous DMSO (Aldrich) containing 20% Pluronic F-127. Then macrophages were loaded with fluo-3 by incubation with 10 μM fluo-3/AM in physiological salt solution (final DMSO concentration, 0.1%) at room temperature for 15 min or with 20 μM Sodium green tetra-acetate for 20 min. A single macrophage of 15–25 μm in diameter was selected and excited at 488 nm by means of a monochromator, whereas fluorescence was detected at 530 ± 15 nm. Only one cell per coverslip was used for experiments. The fluorescence signals were normalized with respect to the resting fluorescence intensity (F_0) and expressed as F/F_0.

Patch–Clamp Measurements. Macrophages were superfused with physiological salt solution containing (in mM): 140 NaCl, 4.5 KCl, 1.2 NaH_2PO_4, 1.13 $MgCl_2$, 1.6 $CaCl_2$, 10 Hepes, 10 glucose, 2 sodium pyruvate, and 0.5% BSA (pH, 7.4) or with high-K^+ physiological salt solution containing 140 mM KCl and 4.5 mM NaCl. The pipette solution contained (in mM) 50 KCl, 65 K^+ glutamate, 10 KH_2PO_4, 2 $MgCl_2$, 1.9 K_2ATP, 0.2 Na_3-GTP, 0.1 EDTA, and 5 Hepes (pH, 7.2) for whole-cell recording, and 150 KCl, 10 EGTA, and 10 Hepes (pH, 7.3) for cell-attached recording. Data were acquired by using an Axopatch 200B amplifier (Axon Instruments, Union City, CA), an A/D converter (PCI-MIO 16-XR-10, National Instruments, Austin, TX) and software (PC.DAQ1.1) developed in our laboratory. The sampling rate was 15 kHz (−3 dB at 5 kHz) for single-channel recordings and 5 kHz (−3 dB at 1 kHz) for whole-cell recordings. All patch–clamp and fluorescence measurements were performed at room temperature (≈22°C). Results are reported as means ± SEM.

Results

Activation of P2Y Receptors. Application of ATP (10 μM) or UTP (10 μM) to human macrophages induced an oscillatory increase in free cytosolic Ca^{2+}, which rapidly reversed after washout (Fig. 1 *A* and *B*). The frequency of the oscillations was in the range 3 to 19 min^{-1}; the mean value was 12.1 ± 0.7 min^{-1} with 10 μM ATP (n = 31) and 11.5 ± 0.7 min^{-1} with 10 μM UTP (n = 6); the small difference was not significant ($P > 0.05$). When ATP was washed out after 30–45 s, the cell was responsive to repeated ATP application. When the application of ATP was prolonged to >3 min, the cells became refractory to repeated ATP-induced Ca^{2+} release.

P2X receptors are virtually insensitive to UTP, whereas some P2Y receptors (for example, $P2Y_2$) show approximately equal sensitivity to ATP and UTP (9, 12). Furthermore, the increase

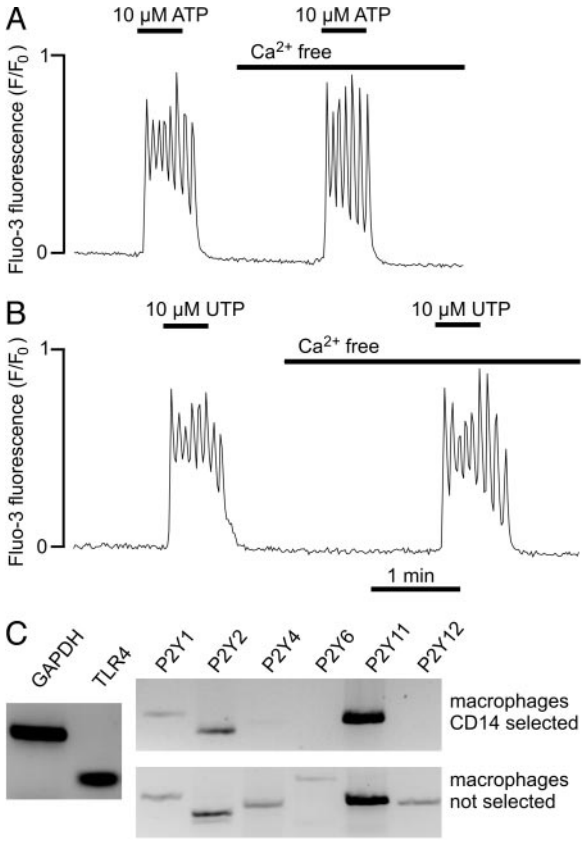

Fig. 1. Ca^{2+} oscillations triggered by activation of P2Y receptors. (*A*) Effects of 10 μM ATP on intracellular Ca^{2+} in a fluo-3-loaded macrophage. (*B*) Effects of 10 μM UTP in a different macrophage. (*C*) Ethidium bromide-stained agarose gel showing RT-PCR products generated from total RNA of macrophages. The controls (*Left*) show the expression of GAPDH and Toll-like receptor 4. The primer sequences are shown in Table 1.

in intracellular Ca^{2+} mediated by the P2X receptors should be abolished in the absence of extracellular Ca^{2+}. However, when the application of ATP (10 μM) or UTP (10 μM) was repeated in Ca^{2+}-free solution, the Ca^{2+} oscillations were virtually unchanged (Fig. 1 *A* and *B*), indicating that the Ca^{2+} oscillations triggered by 10 μM ATP or UTP were mainly due to Ca^{2+} movements between intracellular compartments (Fig. 6, which is published as supporting information on the PNAS web site).

The expression pattern of P2Y receptors was analyzed by RT-PCR. In macrophages generated from purified $CD14^+$ monocytes, we found expression of $P2Y_1$, $P2Y_2$, and $P2Y_{11}$ (Fig. 1*C*), although the amplified $P2Y_1$ signal was relatively weak. In macrophages not subjected to the CD14 purification step, the $P2Y_4$ and $P2Y_6$ receptor subtypes could also be detected. The $P2Y_{11}$ receptor was probably not involved in the Ca^{2+} oscillations because it is insensitive to UTP (9, 17), whereas in our experiments, ATP and UTP were approximately equipotent. To differentiate between $P2Y_1$ and $P2Y_2$ receptors, we studied the effects of ADP, UDP, and 2-methylthio-ATP, which do not activate $P2Y_2$ receptors (9). Only 6 of 12 cells responded to 10 μM ADP (peak F/F_0, 5.8 ± 0.2; n = 6) and only 5 of 10 cells responded to 10 μM UDP (peak F/F_0, 5.6 ± 0.5; n = 5). Furthermore, 10 μM 2-methylthio-ATP exerted a negligible effect or no effect on cytosolic Ca^{2+} (n = 9; data not shown). Taken together, our results suggest that the Ca^{2+} oscillations elicited in macrophages by low nucleotide concentrations were mainly due to activation of $P2Y_2$ receptors.

Application of ATP also induced striking morphological

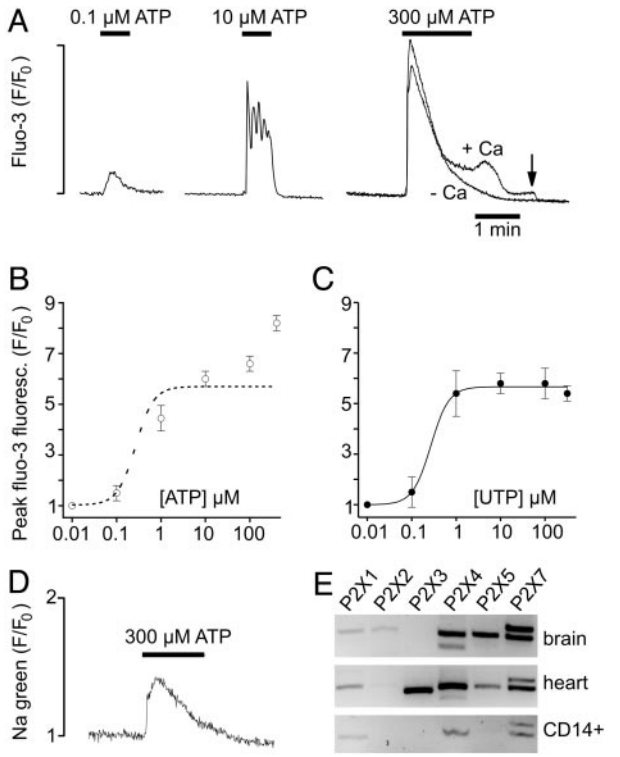

Fig. 2. Concentration dependence of the effects of ATP and UTP. (*A*) Effects of ATP on intracellular Ca^{2+}. The measurement with 300 μM ATP (+Ca) was repeated in the absence extracellular Ca^{2+} (−Ca). The arrow indicates removal of extracellular Ca^{2+}. (*B*) Plot of ATP concentration versus peak intracellular Ca^{2+}. The dotted line is the UTP dose–response curve. (*C*) Plot of UTP concentration versus peak intracellular Ca^{2+}. (*D*) Changes in intracellular Na^+ measured with Sodium green during application of 300 μM ATP. (*E*) RT-PCR products amplified from total RNA of human brain, heart, and CD14-selected macrophages by using primers (Table 1) for P2Y receptors.

changes in macrophages (Fig. 7, which is published as supporting information on the PNAS web site). Time-lapse Movie 1, which is published as supporting information on the PNAS web site, illustrates the characteristic movements of the filopodia exploring the space above the cell soma. Time-lapse Movie 2, which is published as supporting information on the PNAS web site, shows that switching to a superfusate containing 10 μM ATP caused contraction and rounding up of the cells and shortening of the filopodia. Upon washout of ATP, the morphological changes were reversed within 1 min (data not shown). Similar results were obtained in 20 further experiments, both at 37°C and at 22°C. It appears likely that the morphological changes were triggered by the Ca^{2+} oscillations.

Activation of P2X Receptors. To obtain more information on the functional role of P2X receptors, we studied the concentration dependence of the effects of UTP and ATP on peak cytosolic Ca^{2+} (Fig. 2*A*). Because purinoceptors are known to inactivate/desensitize, only the first Ca^{2+} response of a given macrophage to application of nucleotides was used for constructing the dose–response curves (Fig. 2 *B* and *C*). The half-maximal effect of UTP (EC_{50}) was reached at a concentration of 0.3 μM, and the dose–response curve was flat at UTP concentrations of >1 μM (Fig. 2*C*). The effects of UTP probably reflect activation of P2Y receptors. The steep increase in the Ca^{2+} signal between 0.1 and 1 μM UTP was probably due to the amplification of the signal via the G_q-PLC-inositol (1,4,5)-trisphosphate pathway (6, 7, 9).

The dose–response curve for ATP was biphasic and continued to increase for concentrations up to 300 μM (the highest concentration studied), suggesting that macrophages also express P2X receptors and that the dose–response curves of ATP at P2X and P2Y receptors partially overlap. To confirm the expression of P2X receptors, we measured the changes in intracellular Na^+ induced by using the fluorescent indicator Sodium green (Fig. 2*D*). Application of 300 μM ATP produced a transient increase in Sodium green fluorescence. The transient nature of the Na^+ signal was probably due to desensitization (or inactivation) of P2X receptors (12). At higher ATP concentrations, the initial Ca^{2+} spike was followed by a plateau (Fig. 2*A*). The plateau was probably attributable to Ca^{2+} influx through store-operated channels or P2X receptors because it was abolished after removal of extracellular Ca^{2+}.

RT-PCR analysis of $CD14^+$ macrophages showed expression of $P2X_1$, $P2X_4$, and two splice variants of $P2X_7$ (Fig. 2*E*). Control experiments showed that $P2X_2$ receptors could be detected in brain cDNA and $P2X_3$ receptors could be detected in heart cDNA.

Effects of ATP on the Electrical Activity of Human Macrophages. The basic electrical properties of the macrophages were studied by using the patch–clamp technique (Fig. 8, which is published as supporting information on the PNAS web site). To characterize the whole-cell currents activated by ATP, we used a pipette solution containing no added Ca^{2+} and 100 μM of the Ca^{2+} buffer EDTA, which did not prevent changes in intracellular Ca^{2+}. Simultaneous measurement of the current components attributable to P2X and P2Y receptors was performed by stepping the membrane potential back and forth between −80 and 0 mV every 50 ms (Fig. 3*A*). The rationale was that at −80 mV, near the K^+ equilibrium potential (E_K), the current flowing through K^+ channels should be minimized, whereas at 0 mV the current through P2X receptors (a nonselective cation current) should be minimized. Application of 10 μM ATP produced an oscillatory outward current at 0 mV and a transient inward current at −80 mV. Similar results were obtained in eight further experiments, in which the membrane potential was either continuously held at −80 or 0 mV or repetitively switched between the two potentials. The inward current at −80 mV was much smaller during the second application of ATP, probably due to desensitization. The frequency of the current oscillations measured at 0 mV was between 8 and 23 min^{-1}, the mean value was 15 ± 1 min^{-1} (n = 32). Application of 10 μM UTP produced similar current oscillations at 0 mV but no inward current at −80 mV (data not shown).

To acquire further information on the functional consequences of purinoceptor activation, we studied the effects of ATP on the membrane potential of macrophages (Fig. 3*B*). Application of 10 μM ATP gave rise to an initial depolarization, followed by repetitive transient hyperpolarizations with a frequency of 7–16 min^{-1}; the mean value was 9.5 ± 0.9 min^{-1} (n = 11). The membrane potential oscillations subsided within 30 s after washout of ATP. A second application of ATP produced similar oscillations, but the transient depolarization was much smaller than during the first run. In the absence of extracellular Na^+ and Ca^{2+} (replaced by *N*-methyl D-glucamine) application of 10 μM ATP produced no initial depolarization (n = 3; data not shown). Taken together, our findings suggest that the depolarization was most likely induced by flow of cations through P2X receptors. Because $P2X_1$ and $P2X_7$ are relatively insensitive to ATP and $P2X_1$ desensitizes completely in <1 s (12), the inward current was probably mainly carried by $P2X_4$. The repetitive hyperpolarization was probably related to current flow through Ca^{2+}-activated K^+ channels, triggered by cytosolic Ca^{2+} oscillations.

PHYSIOLOGY

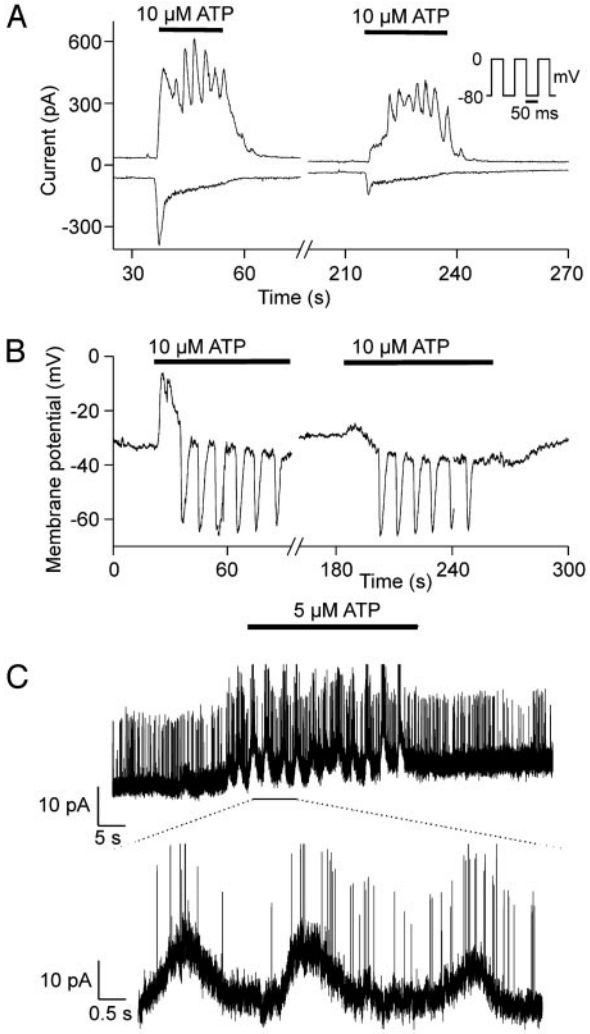

Fig. 3. Oscillations in membrane current and potential. (*A*) Whole-cell voltage–clamp measurement of transmembrane current at 0 mV (upper traces) and −80 mV (lower traces) induced by 10 μM ATP. The membrane potential alternated between the two potentials (see *Inset*) and the mean currents measured after decay of the capacitive transient were plotted. (*B*) Current–clamp measurement of the changes in membrane potential induced by 10 μM ATP. (*C*) Effects of 5 μM ATP on currents measured in a cell-attached patch. The lower trace shows an expanded section of the record. The membrane potential of the cell was held at 0 mV by superfusing the macrophages with high-K^+ solution. The pipette potential was clamped to −80 mV.

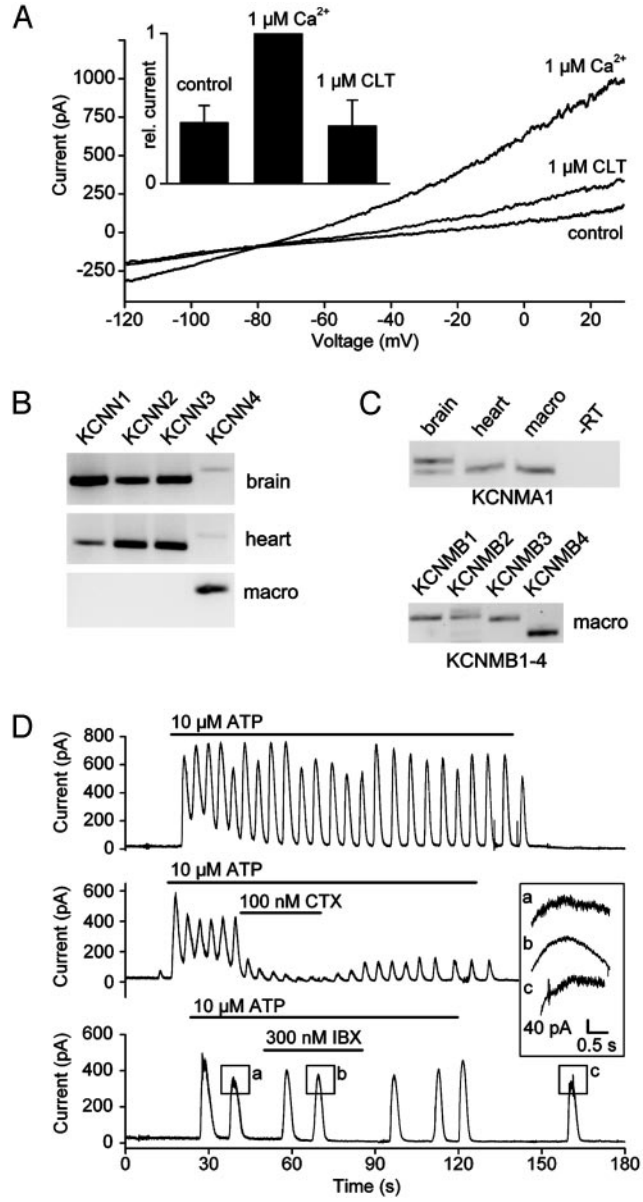

Fig. 4. IK_{Ca} channels in macrophages. (*A*) Whole-cell current measured immediately after rupture of the patch (control), after dialysis of the cell with a pipette solution containing 1 μM Ca^{2+}, and after blockade of IK_{Ca} channels with clotrimazole (CLT). (*Inset*) The relative amplitude of the outward currents measured at +30 mV ($n = 4$) is shown. (*B*) RT-PCR products from human brain, human heart, and CD14-selected macrophages obtained with primers for SK channels (*KCNN1–4*). (*C*) RT-PCR products obtained with primers for the α-subunit (*KCNMA1*) and the β-subunits (*KCNMB1–4*) of BK_{Ca} channels. (*D*) Whole-cell clamp measurement of current oscillations induced by 10 μM ATP under control conditions (upper trace) and during application of charybdotoxin (CTX) or iberiotoxin (IBX). (*Inset*) A higher magnification of the peaks as indicated, is shown. The holding potential was 0 mV. Every cell was exposed to ATP only once.

Identification of Ca^{2+}-Activated K^+ Channels. To characterize the channels involved in the membrane potential oscillations in more detail, we carried out cell-attached recordings with 145 mM K^+ in the bath solution (Fig. 3*C*). Application of 5 μM ATP induced the opening of large conductance channels that were superimposed on the peaks of a slow baseline current oscillation. The amplitude of the baseline oscillations was 9.7 ± 0.9 pA ($n = 3$), and the mean frequency was 14 ± 6 min^{-1} (range, 6–26 min^{-1}). The baseline current oscillations were probably due to the opening of Ca^{2+}-activated K^+ (IK_{Ca}) channels, the amplitude of which was too small to be detected under our experimental conditions. Consistent with our inability to resolve elementary IK_{Ca} currents, the conductance of human IK_{Ca} channels has been reported to be only 5–12 pS in the outward direction (18).

The presence of IK_{Ca} channels was confirmed by whole-cell recordings in which the Ca^{2+} concentration of the pipette solution was buffered to ≈1 μM (Fig. 4*A*). Control current–voltage relations were measured immediately after establishing whole-cell conditions. After 2 min, the outward current at positive potentials and the inward current at negative potentials showed a pronounced increase, due to cell dialysis with the pipette solution. The additional current reversed near E_K and could be inhibited by application of 1 μM clotrimazole, a blocker of SK_{Ca} and IK_{Ca} channels. These findings suggest that, at least at moderately elevated cytosolic Ca^{2+} concentrations, IK_{Ca} channels are responsible for the major part of

the Ca^{2+}-activated K^+ current. RT-PCR analysis of CD14-selected human macrophages confirmed the electrophysiological data. We found that of the four known SK subtypes only SK-4 (*KCNN4*), which corresponds to IK_{Ca}, was expressed in human macrophages (Fig. 4*B*).

The mean elementary conductance of BK channels was 197 ± 5.7 pS ($n = 7$) with symmetrical K^+ (Fig. 9, which is published as supporting information on the PNAS web site). RT-PCR experiments showed that only one splice variant of BK_{Ca} (*KCNMA1*) was expressed in the macrophages (Fig. 4*C*), whereas, with the same primers, two splice variants were found in brain, one showing a 27-aa insertion (GenBank accession no. AY445624). Sequencing of the PCR products showed that the splice variant expressed in macrophages was identical to that published (GenBank accession no. NM_002247).

Surprisingly, we found that all four known β-subunits (*KCNMB1–4*) of BK_{Ca} were expressed in human macrophages (Fig. 4*C*). The β-subunits may serve to modify the Ca^{2+} sensitivity of the channels. Our electrophysiological findings, together with the RT-PCR data, indicate that both BK_{Ca} and IK_{Ca} channels (*KCNMA1* and *KCNN4*) might contribute to the membrane potential oscillations. To assess the relative contribution of these channels, we used iberiotoxin, a specific blocker of BK_{Ca}, and charybdotoxin, a blocker of both BK_{Ca} and IK_{Ca} (Fig. 4*D*). Under control conditions, the membrane potential oscillations were sustained for 2 or more minutes ($n = 4$). Application of 100 nM charybdotoxin reduced the amplitude of the oscillations to 15 ± 3% of control ($n = 4$). Application of 300 nM iberiotoxin caused only a minor (but significant; $P < 0.05$) change in amplitude to 94 ± 3% of control ($n = 3$). In addition, it reduced the noise observed at the peak of the oscillations (Fig. 4*D Inset*), most likely by blocking BK_{Ca} channels. These findings indicate that the Ca^{2+} oscillations were mainly attributable to the opening of IK_{Ca} channels.

Effects of ATP on Expression of IL-6. Next, we studied the effects of the nonhydrolyzable ATP analogue ATPγS on the transcription of IL-6 in CD14-purified human macrophages by using quantitative RT-PCR. The calibration was carried out relative to the housekeeping gene GAPDH. Under control conditions, the transcription of IL-6 was very low. Addition of 10 μM ATPγS for 2 h before isolation of RNA induced an ≈40-fold increase in mRNA for IL-6 (Fig. 5*A*). As a positive control, we applied 100 ng/ml lipopolysaccharide, which increased IL-6 expression ≈1,000-fold. In the presence of 100 μM suramin, which blocks $P2Y_1$, $P2Y_2$, and $P2X_1$ receptors (9, 12, 17), 10 μM ATPγS had no effect on the transcription of IL-6. Because mitogen-activated protein kinases and Ca^{2+}-dependent protein kinase C have been implicated in the release of IL-6 from immunocytes (19, 20), we tested the effects of (*i*) an inhibitor of Ca^{2+}-dependent protein kinase C (Gö6976), (*ii*) an inhibitor of p38 mitogen-activated protein kinase (SB203580), (*iii*) an inhibitor of extracellular signal-related protein kinases 1 and 2 (PD98059) and, in addition, (*iv*) an inhibitor of the NFAT pathway (cyclosporin A). The stimulatory effect of ATPγS on IL-6 expression was not significantly inhibited by these drugs (Fig. 5*A*).

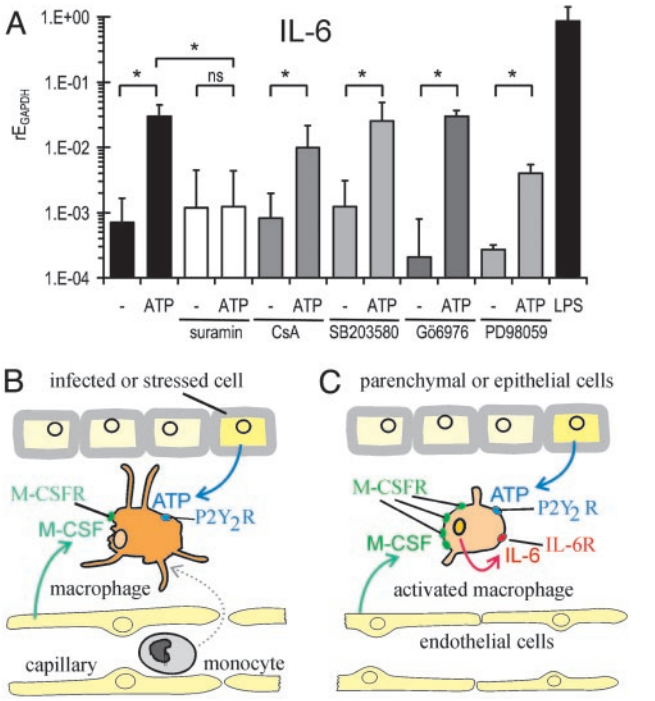

Fig. 5. Expression of IL-6 and the role of extracellular ATP. (*A*) Quantitative RT-PCR analysis of human macrophages from six different donors. Cells were stimulated either with 10 μM ATPγS or with 100 ng·ml^{-1} lipopolysaccharide for 2 h. The inhibitors suramin (100 μM), Gö6976 (1 μM), SB203580 (10 μM), and PD98059 (10 μM) were added 60 min before stimulation with ATPγS. Shown is the expression of IL-6 mRNA expression relative to GAPDH ($rE_{GAPDH} = 1/2^{\Delta Ct}$), with (ATP) and without (−) 2 h exposure to 10 μM ATP. The geometric means and SEM of the logarithm of the relative expression are plotted (*, $P < 0.05$; ns, not significant). (*B* and *C*) Hypothetical scheme of the role of ATP (see text).

Discussion

Ca^{2+} Oscillations. The intracellular Ca^{2+} signals elicited by activation of purinergic receptors were detected by three different approaches: (*i*) single-cell fluorescence measurements with fluo-3, (*ii*) whole-cell recording, and (*iii*) cell-attached patch–clamp recording of Ca^{2+}-activated K^+ channels. The former two methods are "invasive" in the sense that they may have distorted the cytosolic Ca^{2+} signals. The somewhat lower mean frequency of the Ca^{2+} oscillations as compared with the whole-cell current oscillations may be attributable to the additional buffer capacity introduced by the fluorescent Ca^{2+} indicator, which could perturb the kinetics of Ca^{2+} movements between different intracellular compartments. On the other hand, during whole-cell recording, dialysis of the cells with the pipette solution might have eluted some intracellular components. Oscillations in channel activity with a similar frequency were also seen in cell-attached patches, which is a relatively "noninvasive" method. The consistent results obtained with the three approaches, together with the distinct morphological changes observed after application of ATP at 37°C, suggest that nucleotide-induced Ca^{2+} oscillations may also take place *in vivo*.

Our experiments suggest that the Ca^{2+} oscillations initiated by activation of P2Y receptors were mainly due to Ca^{2+} cycling between the endoplasmic reticulum and the cytosol, mediated by inositol (1,4,5)-trisphosphate receptors and a Ca^{2+}-ATPase. In T lymphocytes, Ca^{2+} oscillations have been shown to modulate specific gene expression in a frequency-dependent fashion (21). Thus, the nucleotide-induced Ca^{2+} oscillations described here may switch on the expression of IL-6 and other genes in macrophages, depending on the amplitude and frequency of the Ca^{2+} oscillations. Oscillatory changes in Ca^{2+} may be advantageous for receptor-mediated signal transduction by increasing signaling specificity, by preventing desensitization, and by increasing the ability of small Ca^{2+} signals to activate transcription factors (21, 22).

Membrane Potential Oscillations. Our measurements suggest that the transient depolarization was mainly due to activation of $P2X_4$ receptors and the repetitive hyperpolarization was mainly due to activation of $P2Y_2$ receptors. Consistent with our results, a very recent study (23) of the effects of ATP on NR8383 cells (a rat

PHYSIOLOGY

alveolar macrophage-derived cell line) showed a transient inward current followed by an outward current carried by apamin-sensitive K^+ channels. These effects were attributed to activation of $P2X_4$ and $P2Y_1$ or $P2Y_2$ receptors.

We have shown that, despite their small conductance in the outward direction (18), activation of IK_{Ca} channels (*KCNN4*) represents the major mechanism underlying the membrane potential oscillations in macrophages, at least during moderate elevation of intracellular Ca^{2+}. Evidence for functional expression of IK_{Ca} channels has also been obtained in cultured microglial cells (24–26). IK_{Ca} channels show a relatively high Ca^{2+} affinity, which permits rapid responses to physiological fluctuations of submembrane Ca^{2+} (27). Our cell-attached recordings and the PCR analysis show that BK_{Ca} channels (*KCNMA1* and *KCNMB1–4*) are also functionally expressed in macrophages, but the low sensitivity of the membrane potential oscillations to iberiotoxin suggests that they play only a minor role, if any, in mediating the effects of low concentrations of ATP. Interestingly, "spontaneous" hyperpolarizations bearing some resemblance with the membrane potential oscillations described here were also found in guinea pig peritoneal macrophages (28).

The functional significance of the oscillatory changes in membrane potential is not yet clear. One possibility is that the hyperpolarization caused by the opening of Ca^{2+}-activated K^+ channels may be required to maintain the driving force for Ca^{2+} influx through ligand-gated (P2X) channels, or through transient receptor potential channels (27, 29), in face of a P2X-receptor mediated cation influx. A second possibility is that membrane hyperpolarization generated through activation of BK_{Ca} or IK_{Ca} channels may increase the activity of NADPH oxidase, the enzyme responsible for generating reactive oxygen species during respiratory bursts (26, 30).

ATP as a Danger Signal. We have shown that 10 μM ATP induces an $\approx$40-fold increase in the transcription of IL-6. It is likely that this resulted in increased release of IL-6 (31), but it cannot be excluded that some IL-6 accumulated in the cytosol and required an additional stimulus for release. The finding that the response was abolished by application of 100 μM suramin, together with our RT-PCR analysis, suggests that the effects of ATP on IL-6 expression were mainly attributable to activation of $P2Y_2$ receptors. The lack of effect of specific inhibitors suggests that the NFAT pathway, Ca^{2+}-dependent protein kinase C, and the mitogen-activated protein kinase pathway were not required for signal transduction.

Because ATP is not only liberated from lytic cells but also secreted during metabolic or mechanical stress (8), it may represent a danger signal that promotes the development of an inflammatory response. We propose that, in the framework of the infectious nonself model (1–3) and the danger model (4, 5), micromolar concentrations of ATP may participate in the following sequence of events leading to activation of the immune response (Fig. 5 *B* and *C*): (*i*) monocytes cross the endothelial barrier and infiltrate the infected tissue, attracted by M-CSF (32, 33) secreted by fibroblasts (33) and endothelial cells, and by ATP (11) released by infected cells (Fig. 5*B*); (*ii*) M-CSF induces differentiation of infiltrated monocytes to macrophages; (*iii*) ATP promotes the transcription and release of IL-6 in macrophages (Fig. 5*C*); (*iv*) IL-6 released from macrophages and fibroblasts (33) promotes further maturation of macrophages (34) by up-regulating the expression of M-CSF receptor (33); and (*v*) IL-6 stimulates terminal differentiation of T and B lymphocytes (35). In summary, we propose that ATP acts as a danger signal and initiates a complex sequence of events leading to enhancement of the immune response.

In agreement with the proposed role of ATP as a danger signal inducing the expression of IL-6, the reaction of IL-6 knockout mice to sterile tissue damage was dramatically reduced as compared with wild-type controls (36). Furthermore, in agreement with the proposed role of the innate immune system in controlling the adaptive immune response (1), the defense against viral or bacterial infection was also drastically impaired in IL-6 knockout mice (36). Because infectious nonself signals (mediated by Toll-like receptors and other pattern recognition receptors) and danger signals (mediated by purinergic and other receptors) converge on macrophages, we propose that it is in fact the combination of the two types of signals that determines the quality and the extent of the activation of the innate immune system.

We thank C. Barett, H. Bykow, G. Schlichthörl, R. Graf, and K. Schneider for technical assistance. This work was supported by Deutsche Forschungsgemeinschaft Grants SFB593 and Da 177/8-1.

1. Janeway, C. A., Jr., & Medzhitov, R. (2002) *Annu. Rev. Immunol.* **20,** 197–216.
2. Bretscher, P. A. (1999) *Proc. Natl. Acad. Sci. USA* **96,** 185–190.
3. Medzhitov, R. & Janeway, C. A., Jr. (2002) *Science* **296,** 298–300.
4. Gallucci, S. & Matzinger, P. (2001) *Curr. Opin. Immunol.* **13,** 114–119.
5. Matzinger, P. (2002) *Science* **296,** 301–305.
6. Communi, D., Janssens, R., Suarez-Huerta, N., Robaye, B. & Boeynaems, J. M. (2000) *Cell Signalling* **12,** 351–360.
7. Di Virgilio, F., Chiozzi, P., Ferrari, D., Falzoni, S., Sanz, J. M., Morelli, A., Torboli, M., Bolognesi, G. & Baricordi, O. R. (2001) *Blood* **97,** 587–600.
8. Lazarowski, E. R., Boucher, R. C. & Harden, T. K. (2003) *Mol. Pharmacol.* **64,** 785–795.
9. Ralevic, V. & Burnstock, G. (1998) *Pharmacol. Rev.* **50,** 413–492.
10. Goepfert, C., Sundberg, C., Sevigny, J., Enjyoji, K., Hoshi, T., Csizmadia, E. & Robson, S. (2001) *Circulation* **104,** 3109–3115.
11. Honda, S., Sasaki, Y., Ohsawa, K., Imai, Y., Nakamura, Y., Inoue, K. & Kohsaka, S. (2001) *J. Neurosci.* **21,** 1975–1982.
12. North, R. A. (2002) *Physiol. Rev.* **82,** 1013–1067.
13. Ferrari, D., Chiozzi, P., Falzoni, S., Dal Susino, M., Melchiorri, L., Baricordi, O. R. & Di Virgilio, F. (1997) *J. Immunol.* **159,** 1451–1458.
14. Fairbairn, I. P., Stober, C. B., Kumararatne, D. S. & Lammas, D. A. (2001) *J. Immunol.* **167,** 3300–3307.
15. Alonso-Torre, S. R. & Trautmann, A. (1993) *J. Biol. Chem.* **268,** 18640–18647.
16. Albuquerque, C., Oliveira, S. M., Coutinho-Silva, R., Oliveira-Castro, G. M. & Persechini, P. M. (1993) *Am. J. Physiol.* **265,** C1663–C1673.
17. von Kugelgen, I. & Wetter, A. (2000) *Naunyn-Schmiedeberg's Arch. Pharmacol.* **362,** 310–323.
18. Ishii, T. M., Silvia, C., Hirschberg, B., Bond, C. T., Adelman, J. P. & Maylie, J. (1997) *Proc. Natl. Acad. Sci. USA* **94,** 11651–11656.
19. Tuyt, L. M., Dokter, W. H., Birkenkamp, K., Koopmans, S. B., Lummen, C., Kruijer, W. & Vellenga, E. (1999) *J. Immunol.* **162,** 4893–4902.
20. Shigemoto-Mogami, Y., Koizumi, S., Tsuda, M., Ohsawa, K., Kohsaka, S. & Inoue, K. (2001) *J. Neurochem.* **78,** 1339–1349.
21. Dolmetsch, R. E., Xu, K. & Lewis, R. S. (1998) *Nature* **392,** 933–936.
22. Lewis, R. S. (2001) *Annu. Rev. Immunol.* **19,** 497–521.
23. Bowler, J. W., Bailey, R. J., North, R. A. & Surprenant, A. (2003) *Br. J. Pharmacol.* **140,** 567–575.
24. Eder, C. (1998) *Am. J. Physiol.* **275,** C327–C342.
25. Schilling, T., Repp, H., Richter, H., Koschinski, A., Heinemann, U., Dreyer, F. & Eder, C. (2002) *Neuroscience* **109,** 827–835.
26. Khanna, R., Roy, L., Zhu, X. & Schlichter, L. C. (2001) *Am. J. Physiol.* **280,** C796–C806.
27. Cahalan, M. D., Wulff, H. & Chandy, K. G. (2001) *J. Clin. Immunol.* **21,** 235–252.
28. Gallin, E. K., Wiederhold, M. L., Lipsky, P. E. & Rosenthal, A. S. (1975) *J. Cell Physiol.* **86,** Suppl. 2, 653–661.
29. Jiang, X., Newell, E. W. & Schlichter, L. C. (2003) *J. Biol. Chem.* **278,** 42867–42876.
30. Schmid-Antomarchi, H., Schmid-Alliana, A., Romey, G., Ventura, M. A., Breittmayer, V., Millet, M. A., Husson, H., Moghrabi, B., Lazdunski, M. & Rossi, B. (1997) *J. Immunol.* **159,** 6209–6215.
31. Bost, K. L. & Mason, M. J. (1995) *J. Immunol.* **155,** 285–296.
32. Dai, X. M., Ryan, G. R., Hapel, A. J., Dominguez, M. G., Russell, R. G., Kapp, S., Sylvestre, V. & Stanley, E. R. (2002) *Blood* **99,** 111–120.
33. Chomarat, P., Banchereau, J., Davoust, J. & Palucka, A. K. (2000) *Nat. Immunol.* **1,** 510–514.
34. Mitani, H., Katayama, N., Araki, H., Ohishi, K., Kobayashi, K., Suzuki, H., Nishii, K., Masuya, M., Yasukawa, K., Minami, N. & Shiku, H. (2000) *Br. J. Haematol.* **109,** 288–295.
35. Diehl, S. & Rincon, M. (2002) *Mol. Immunol.* **39,** 531–536.
36. Kopf, M., Baumann, H., Freer, G., Freudenberg, M., Lamers, M., Kishimoto, T., Zinkernagel, R., Bluethmann, H. & Kohler, G. (1994) *Nature* **368,** 339–342.